Cell Reports

Report

Heterosynaptic Structural Plasticity on Local Dendritic Segments of Hippocampal CA1 Neurons

Graphical Abstract

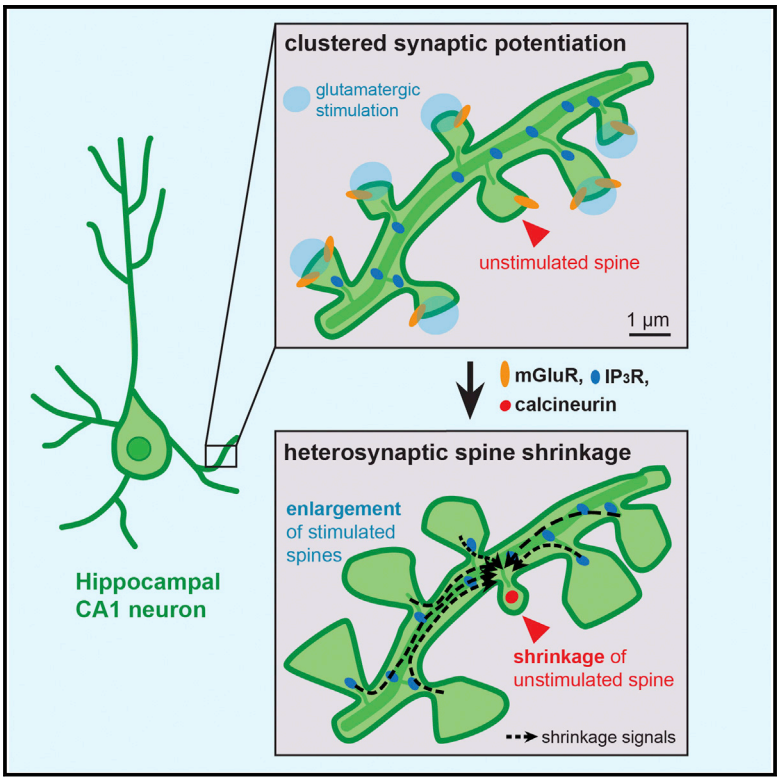

Authors

Won Chan Oh, Laxmi Kumar Parajuli, Karen Zito

Correspondence

kzito@ucdavis.edu

In Brief

Plasticity of neuronal structure, such as the growth and retraction of dendritic spines, is thought to support neural circuit remodeling early in development and during learning in the adult. Oh et al. identify a novel role for competitive interactions between neighboring synapses in driving structural and functional changes in excitatory synapses on dendritic spines in the cerebral cortex.

Highlights

- Local competition between hippocampal synapses drives synaptic structural changes
- Structural potentiation of multiple spines drives shrinkage of nearby inactive spines
- Heterosynaptic spine shrinkage is tightly coupled to synaptic weakening
- Heterosynaptic spine shrinkage requires activation of calcineurin, IP_3Rs, and mGluRs

Oh et al., 2015, Cell Reports *10*, 162–169
January 13, 2015
http://dx.doi.org/10.1016/j.celrep.2014.12.016

CellPress

OPEN ACCESS
CellPress

Cell Reports
Report

Heterosynaptic Structural Plasticity on Local Dendritic Segments of Hippocampal CA1 Neurons

Won Chan Oh,[1,2] Laxmi Kumar Parajuli,[1] and Karen Zito[1,*]
[1]Center for Neuroscience, University of California Davis, Davis, CA 95616, USA
[2]Present address: Max Planck Florida Institute for Neuroscience, Jupiter, FL 33458, USA
*Correspondence: kzito@ucdavis.edu
http://dx.doi.org/10.1016/j.celrep.2014.12.016

SUMMARY

Competition between synapses contributes to activity-dependent refinement of the nervous system during development. Does local competition between neighboring synapses drive circuit remodeling during experience-dependent plasticity in the cerebral cortex? Here, we examined the role of activity-mediated competitive interactions in regulating dendritic spine structure and function on hippocampal CA1 neurons. We found that high-frequency glutamatergic stimulation at individual spines, which leads to input-specific synaptic potentiation, induces shrinkage and weakening of nearby unstimulated synapses. This heterosynaptic plasticity requires potentiation of multiple neighboring spines, suggesting that a local threshold of neural activity exists beyond which inactive synapses are punished. Notably, inhibition of calcineurin, IP_3Rs, or group I metabotropic glutamate receptors (mGluRs) blocked heterosynaptic shrinkage without blocking structural potentiation, and inhibition of Ca^{2+}/calmodulin-dependent protein kinase II (CaMKII) blocked structural potentiation without blocking heterosynaptic shrinkage. Our results support a model in which activity-induced shrinkage signal, and not competition for limited structural resources, drives heterosynaptic structural and functional depression during neural circuit refinement.

INTRODUCTION

Plasticity of neuronal structure, such as the growth and retraction of individual dendritic spines, is thought to support experience-dependent neural circuit remodeling (Bosch and Hayashi, 2012; Holtmaat and Svoboda, 2009). Indeed, as neural circuits are modified during learning, their optimization and fine-tuning involves the weakening and loss of superfluous synaptic connections. Manipulations leading to experience-dependent plasticity of neuronal circuits also increase the rate of spine shrinkage and elimination (Holtmaat et al., 2006; Tschida and Mooney, 2012; Xu et al., 2009; Yang et al., 2009). Yet it remains unclear how neural activity drives the selective shrinkage and loss of individual dendritic spines in response to sensory experience.

Several studies have established that activity-dependent spine shrinkage and elimination are associated with long-term depression (LTD) of synaptic transmission (Nägerl et al., 2004; Zhou et al., 2004), which can occur at individual dendritic spines via an input- and synapse-specific mechanism (Oh et al., 2013) or via a spreading depression (Hayama et al., 2013; Wiegert and Oertner, 2013). In this study, we hypothesized that competitive interactions with neighboring synapses may also play a major role in the structural plasticity associated with synaptic weakening, as it is well-established that stimuli that induce long-term potentiation (LTP) of synaptic strength in one population of synapses can induce heterosynaptic LTD at inactive synapses on the same cell (Abraham and Goddard, 1983; Coussens and Teyler, 1996; Lo and Poo, 1991; Lynch et al., 1977; Scanziani et al., 1996). Intriguingly, ultrastructural studies have shown that LTP-inducing theta-burst stimuli lead to increased spine sizes and decreased spine densities in the hippocampus (Bourne and Harris, 2011) and motor skill training leads to increased numbers of multiple-synapse boutons and decreased size of neighboring spines in the cerebellum (Lee et al., 2013), suggesting that heterosynaptic plasticity may also operate at the level of synaptic structure.

Here, we used two-photon glutamate uncaging and time-lapse imaging of dendritic spines and fluorescently labeled surface α-amino-3-hydroxy-5-methyl-4-isoxazolepropionic acid receptors (AMPARs) to investigate the role of competitive interactions between synapses in driving structural and functional synaptic plasticity. We show that high-frequency stimulation of individual dendritic spines, which leads to input-specific synaptic potentiation, induces shrinkage and synaptic weakening of nearby unstimulated spines. Heterosynaptic structural plasticity was restricted to local dendritic segments and only came into play following strengthening of multiple neighboring synapses, indicating a local activity threshold that when exceeded leads to shrinkage of nearby inactive spines. Furthermore, heterosynaptic shrinkage requires calcineurin, IP_3R, and group I metabotropic glutamate receptor (mGluR) activation, but not Ca^{2+}/calmodulin-dependent protein kinase II (CaMKII)-dependent structural potentiation of stimulated spines. Our data support a model in which activation of a cluster of synapses leads to the generation of an activity-induced signal that acts through calcineurin and IP_3Rs to drive the shrinkage and depression of nearby inactive synapses.

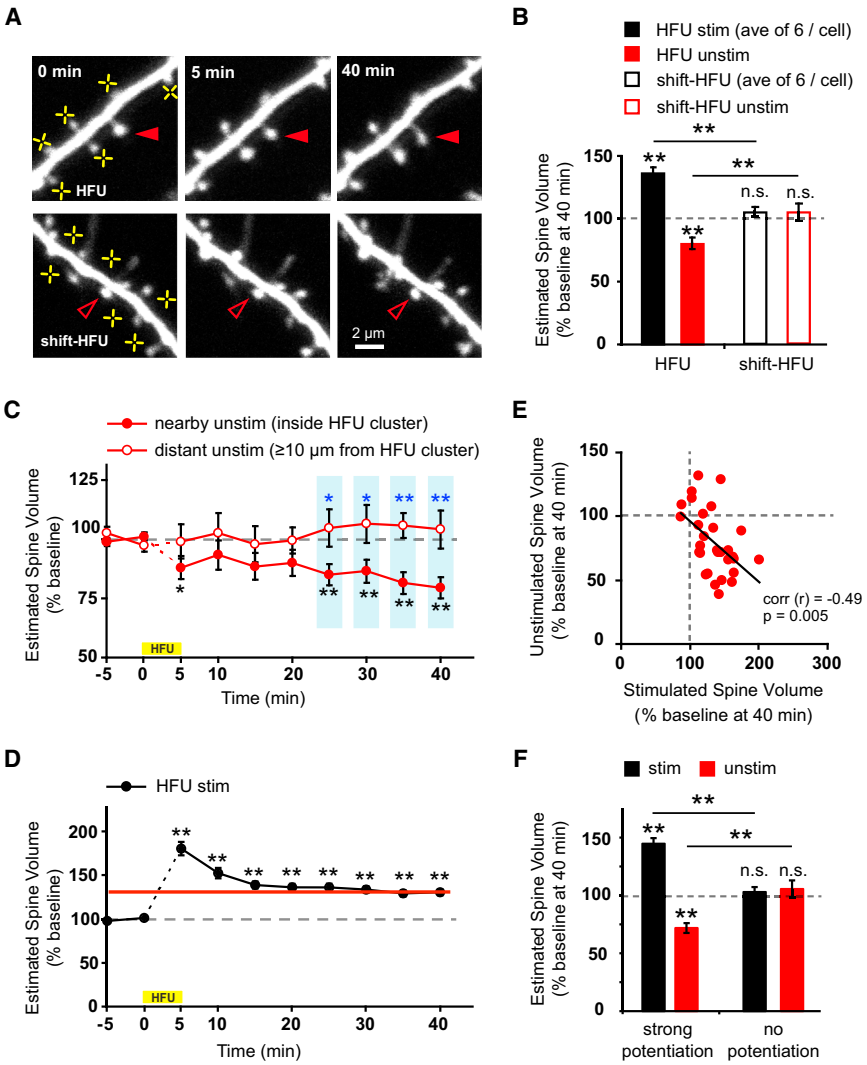

Figure 1. Structural Potentiation of Multiple Spines on a Single Dendritic Segment Induces Structural Depression of Nearby Unstimulated Spines

(A) Images of dendrites from EGFP-transfected CA1 neurons (13–18 DIV) exposed to high-frequency uncaging (HFU; yellow crosses). A nearby unstimulated spine (filled red arrowheads) shrank following HFU stimulation of multiple neighboring spines. In contrast, heterosynaptic shrinkage was not observed at an inactive spine (open red arrowheads) following shifted HFU stimulation.

(B) Structural potentiation of multiple neighboring spines (black bar; 31 cells, average six spines per cell; $p < 0.01$) decreased the size of nearby unstimulated spines compared with baseline (red bar; 31 spines; $p < 0.01$); in contrast, neither neighboring (open black bar; 15 cells, average eight spines per cell; $p = 0.1$) nor unstimulated spines (open red bar, 15 spines; $p = 0.3$) showed changes in size following shifted HFU stimulation.

(C) Time course of heterosynaptic spine shrinkage. Unstimulated spines inside the cluster (3.2 ± 0.6 μm from HFU-stimulated spines; filled red circles; 31 spines) of stimulated neighbors shrank as compared to baseline ($p < 0.01$) or to distant unstimulated spines (≥10 μm from HFU-stimulated spines; $p < 0.05$; blue asterisks) that did not shrink (open red circles; 12 spines; $p > 0.3$ at all post-HFU time points).

(D) Time-course of homosynaptic spine enlargement. Stimulated spines (black circles; 43 cells, average 6.3 ± 0.1 stimulated spines per cell) increased in size in response to HFU stimulation ($p < 0.01$ at all post-HFU time points).

(E) An inverse correlation was found between the magnitude of structural potentiation of stimulated spines (average of all stimulated spines) and the magnitude of shrinkage of inside cluster unstimulated spines on the same dendrites (31 cells; $r = -0.49$, $p < 0.01$).

(F) When HFU-induced structural potentiation of neighboring spines was successful (left black bar; 24 cells, $p < 0.01$), inside cluster unstimulated spines shrank (left red bar; $p < 0.01$); however, shrinkage of inside cluster unstimulated spines was not observed (right red bar; seven cells, $p = 0.49$) when HFU did not lead to potentiation of neighboring spines (HFU failure, right black bar, $p = 0.53$).

Error bars represent SEM.

RESULTS

Structural Potentiation of Multiple Spines on a Single Dendritic Segment Induces Structural Depression of Nearby Unstimulated Spines

To directly test whether competition between neighboring spines could contribute to the spine shrinkage and loss observed during experience-dependent plasticity, we examined whether activity-dependent structural potentiation of dendritic spines leads to shrinkage of nearby inactive spines. We used two-photon glutamate uncaging to stimulate multiple individual dendritic spines with a high-frequency uncaging (HFU) protocol (30 pulses of 1 ms duration at 2 Hz) that induces long-term spine enlargement (Hill and Zito, 2013) and monitored the consequences on the size of nearby unstimulated spines. Remarkably, we found that long-term structural potentiation of a cluster of spines (on average six) induced long-lasting heterosynaptic shrinkage (21% ± 4% decrease) of a nearby unstimulated spine on the same dendritic segment (Figures 1A–1D). Unstimulated spines shrank to a similar extent without regard to their initial size (Figure S1A). Shrinkage of unstimulated spines was not due to glutamate spillover from the clustered glutamate uncaging because unstimulated spines on dendrites exposed to a shifted HFU stimulus, which released the same amount of glutamate at a similar distance away without causing structural potentiation of neighboring spines, did not shrink (Figures 1A and 1B; Figure S1B). Together, these results demonstrate that potentiation of multiple spines on a single dendritic segment can lead to shrinkage of inactive spines via heterosynaptic interactions.

If competitive interactions drive spine shrinkage, we would expect an inverse correlation between the degree of structural enhancement and the extent of heterosynaptic shrinkage.

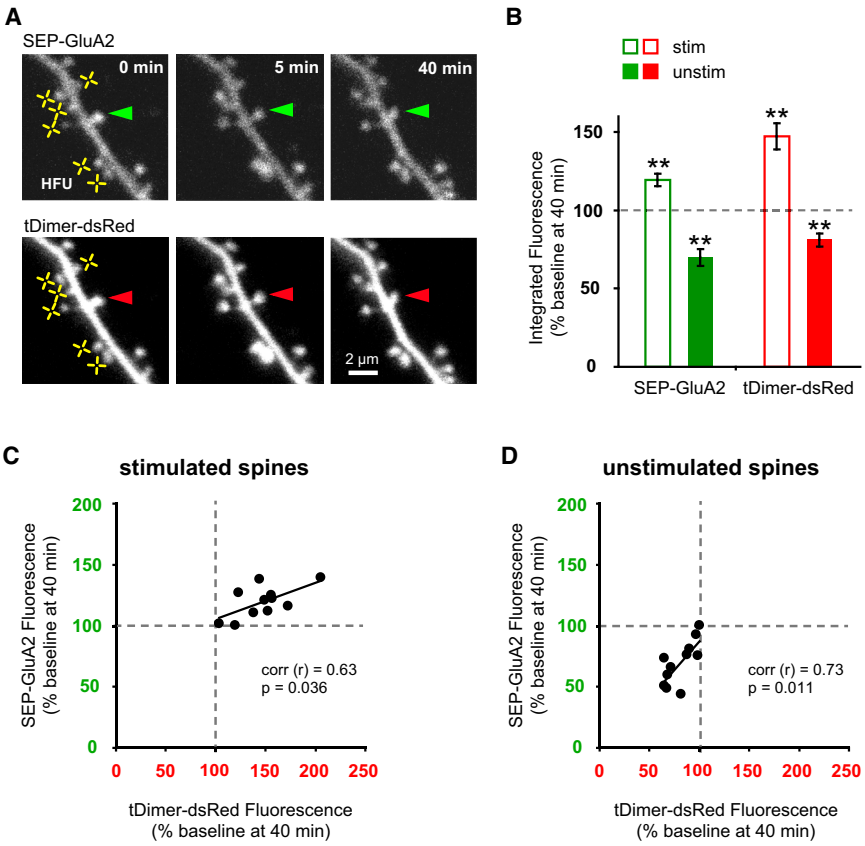

Figure 2. Heterosynaptic Spine Shrinkage Is Tightly Coupled to Synaptic Weakening

(A) Images of a dendrite from a CA1 neuron co-transfected with SEP-GluA2 and tDimer-dsRed. Fluorescence of SEP-GluA2 (top row) and tDimer-dsRed (bottom row) decreased in an unstimulated spine (arrowheads) following HFU-stimulation (yellow crosses) of multiple neighboring spines.

(B) SEP-GluA2 fluorescence increased (open green bar; 11 cells, average six spines per cell; $p < 0.01$) along with spine size (open red bar; $p < 0.01$) in HFU-stimulated spines; SEP-GluA2 fluorescence decreased (solid green bar; 11 spines; $p < 0.01$) along with spine size (solid red bar; $p < 0.01$) in nearby unstimulated spines.

(C) Increases in tDimer-dsRed and SEP-GluA2 fluorescence intensity were tightly correlated in stimulated spines ($r = 0.63$; $p < 0.05$) in response to HFU.

(D) Decreases in tDimer-dsRed and SEP-GluA2 fluorescence intensity were tightly correlated in unstimulated spines ($r = 0.73$; $p < 0.05$) following potentiation of multiple neighboring spines.

Error bars represent SEM.

Such an inverse correlation has been shown between homosynaptic LTP and heterosynaptic LTD (Royer and Paré, 2003). As expected, we observed a significant inverse correlation between homosynaptic spine enlargement and heterosynaptic spine shrinkage (Figure 1E; Figures S1C and S1D). Indeed, a decrease in size (28% ± 4% decrease) of unstimulated spines was observed only when the neighboring cluster of stimulated spines successfully (>115% average increase) underwent structural potentiation (Figure 1F). These data strongly support that competitive interactions between neighboring spines lead to heterosynaptic spine shrinkage.

Heterosynaptic Spine Shrinkage Is Tightly Coupled to Synaptic Weakening

To address whether heterosynaptic spine shrinkage is accompanied by synaptic weakening, we combined glutamate uncaging with two-photon imaging of surface AMPARs fused with superecliptic pHluorin (SEP; Miesenböck et al., 1998). Previous studies have reported that SEP-GluA2 fluorescence is a reliable marker of activity-dependent AMPAR endocytosis (Ashby et al., 2004; Lin and Huganir, 2007) and that LTP-inducing stimuli increase SEP-GluA2 levels in dendritic spines (Kopec et al., 2006). Therefore, we cotransfected CA1 neurons with tDimer-dsRed and SEP-GluA2 and examined both structural and functional heterosynaptic plasticity.

Following induction of heterosynaptic structural plasticity, we monitored the consequences on synaptic strength using SEP-GluA2 fluorescence (Figure 2). As in Figure 1, we observed that unstimulated spines decreased in size in response to long-term structural potentiation of a cluster of neighboring spines. Associated with spine structural plasticity, we found that SEP-GluA2 fluorescence decreased at unstimulated spines and increased at HFU-stimulated spines (Figures 2A and 2B). Notably, SEP-GluA2 expression levels were positively correlated with spine size (Figure S2A), and increases and decreases in SEP-GluA2 and tDimer-dsRed fluorescence were highly correlated in both stimulated and unstimulated spines (Figures 2C and 2D). Strong inverse correlations were observed in both structural and functional heterosynaptic plasticity (Figures S2B and S2C). Thus, potentiation of multiple neighboring spines leads to heterosynaptic spine shrinkage and functional depression at nearby unstimulated spines.

Heterosynaptic Spine Shrinkage Requires Close Physical Proximity to Multiple Potentiated Spines

What are the constraints on the stimulation paradigms that induce heterosynaptic spine shrinkage? We examined how many dendritic spines needed to potentiate in order to trigger heterosynaptic shrinkage of nearby unstimulated spines. Further analysis of the data from HFU at multiple spines (on average six) revealed that heterosynaptic spine shrinkage occurred only after the structural potentiation of more than three spines (Figure 3A). Indeed, following structural potentiation of a single spine or three spines, unstimulated spines did not shrink (Figures 3B and 3C). These results suggest that a minimum of four structurally potentiated spines is required for heterosynaptic shrinkage.

To address the spatial constraints on heterosynaptic structural plasticity, we examined the relationship between heterosynaptic shrinkage and average distance to the stimulated neighboring

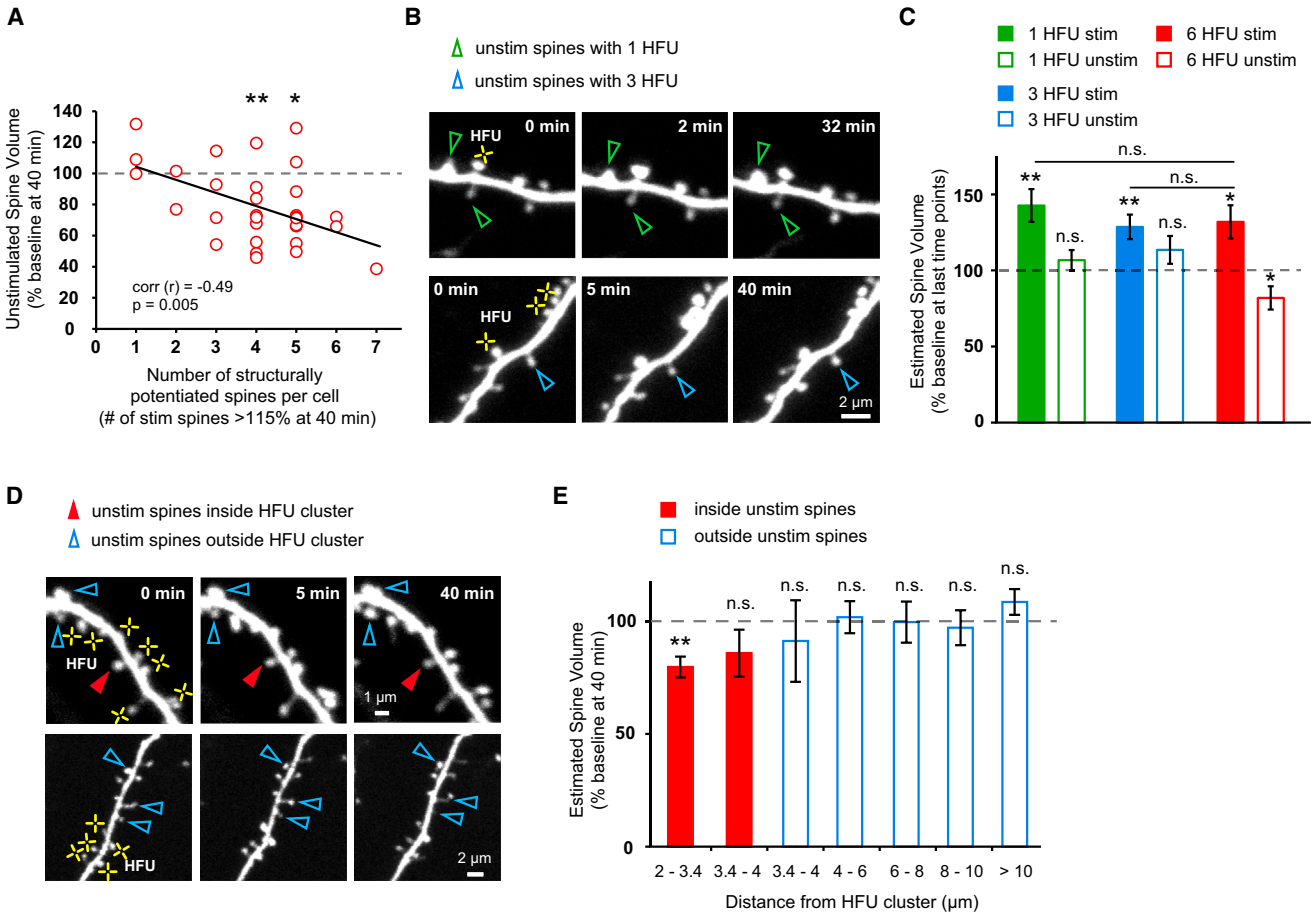

Figure 3. Heterosynaptic Spine Shrinkage Requires Close Physical Proximity to Multiple Potentiated Spines

(A) Shrinkage of unstimulated spines was not observed on those cells for which HFU led to structural potentiation (>115% of baseline at 40 min) of less than four spines; in contrast, when four or more spines potentiated, unstimulated spines shrank (four spines, $p < 0.01$; five spines, $p < 0.05$). Notably, an inverse correlation was found between the number of potentiated spines and the magnitude of shrinkage of unstimulated spines (31 cells, $r = -0.49$, $p = 0.005$).

(B) Images of a dendrite from an EGFP-transfected neuron exposed to one (top row) and three (bottom row) HFU (yellow crosses). Neither single nor triple HFU induced shrinkage of nearby unstimulated spines.

(C) Single (green bar; 25 cells; one spine per cell; $p < 0.01$) or triple (blue bar; ten cells, three spines per cell; $p < 0.01$) HFU increased the size of stimulated spines; however, nearby unstimulated spines did not shrink (open green bar, 50 spines, $p = 0.32$; open blue bar, ten spines, $p = 0.17$). Importantly, the magnitude of spine enlargement by single and triple HFU was indistinguishable (single, $p = 0.56$; triple, $p = 0.81$) from that observed to induce shrinkage of unstimulated spines (red bar; 11 cells, six spines per cell; $p < 0.05$).

(D) Images of dendrites from EGFP-transfected CA1 neurons exposed to multiple HFU stimuli (yellow crosses). An unstimulated spine located within the cluster of HFU-stimulated spines (filled red arrowheads) decreased in size; in contrast, neither unstimulated spines located outside, but directly adjacent to the HFU-stimulated cluster (top row), nor distant unstimulated spines (bottom row) shrank.

(E) Unstimulated spines located closest (2–3.4 µm) to and inside the HFU cluster decreased in size (red bar; 21 spines; $p < 0.01$), whereas those located inside the cluster but 3.4–4 µm from stimulated spines showed no significant shrinkage (red bar; 9 spines; $p = 0.19$). Unstimulated spines located outside of the HFU-stimulated cluster did not shrink (3.4–4 µm, 6 spines, $p = 0.62$; 4–6 µm, 30 spines, $p = 0.9$; 6–8 µm, 23 spines, $p = 0.89$; 8–10 µm, 22 spines, $p = 0.63$; > 10 µm, 25 spines, $p = 0.2$). "inside unstim" data from Figure 1B.

Error bars represent SEM.

spines. We found that unstimulated spines within the cluster that underwent heterosynaptic shrinkage were on average closer (<3.4 µm) to the stimulated spines than those that showed no significant shrinkage inside the cluster (3.4–4 µm) and outside the cluster (>3.4 µm; Figures 3D and 3E). Furthermore, we found that heterosynaptic shrinkage was not related to the magnitude of potentiation of the nearest stimulated spines (Figure S3). Together, our data suggest that heterosynaptic regulation is mediated locally on individual dendritic segments and strongly support a local activity threshold that when exceeded leads to punishment of nearby inactive synapses.

Heterosynaptic Spine Shrinkage Requires Calcineurin, IP_3Rs, and Group I mGluRs, but Not CaMKII

What might constitute a local heterosynaptic shrinkage mechanism? To address whether the shrinkage of inactive spines

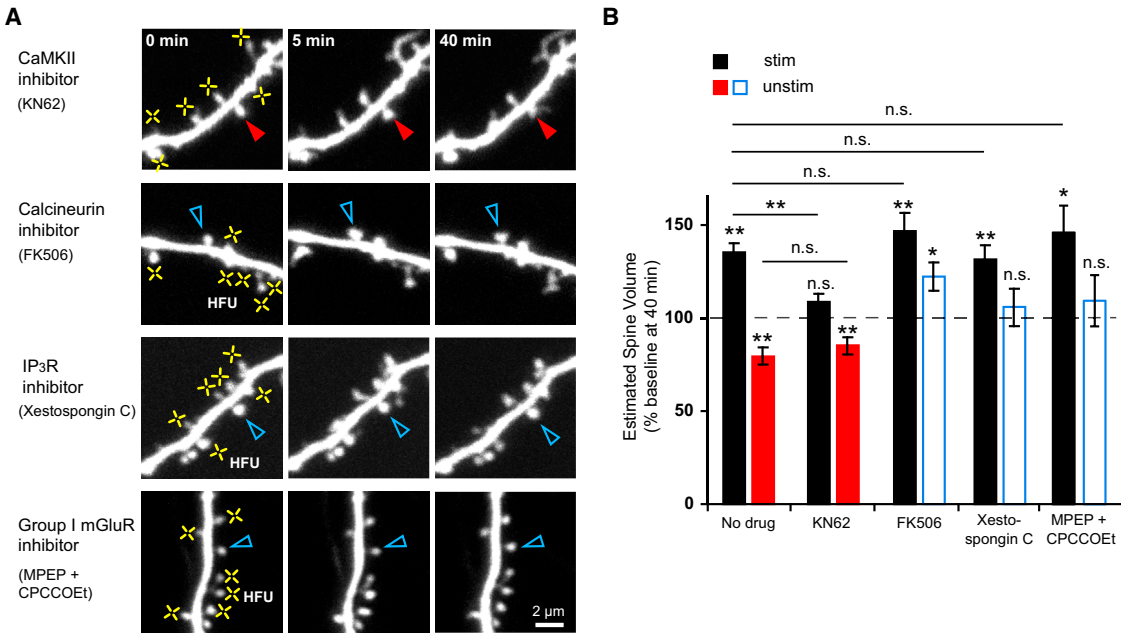

Figure 4. Heterosynaptic Spine Shrinkage Requires Signaling through Calcineurin, IP_3Rs, and Group I mGluRs, but Not CaMKII

(A) Images of dendrites from EGFP-transfected neurons exposed to multiple HFU (yellow crosses) in the presence of inhibitors of CaMKII (KN62, 10 μM), calcineurin (FK506, 2 μM), IP_3Rs (Xesto C, 1 μM), or group I mGluRs (MPEP, 15 μM and CPCCOEt, 45 μM).

(B) Inhibition of CaMKII with KN62 blocked structural potentiation of stimulated spines (black bar; 13 cells; $p = 0.067$) but did not block heterosynaptic shrinkage (red bar; 13 spines; $p < 0.01$). In contrast, inhibition of calcineurin with FK506 (blue bar; 13 spines, $p < 0.05$), IP_3Rs with Xesto C (blue bar; 11 spines, $p = 0.58$), or group I mGluRs with MPEP and CPCCOEt (blue bar; ten spines, $p = 0.51$) blocked heterosynaptic shrinkage without affecting HFU-induced spine enlargement (black bars; FK506, 13 cells, $p < 0.01$; Xesto C, 11 cells, $p < 0.01$; MPEP and CPCCOEt, ten cells, $p < 0.05$), which was not different from that observed without drug (far left black bar; versus FK506, $p = 0.24$; versus Xesto C, $p = 0.66$; versus MPEP and CPCCOEt, $p = 0.49$). "No drug" data from Figure 1B.

Error bars represent SEM.

depends on competition with neighboring stimulated spines for limited structural resources, or whether it is caused by spread of an activity-induced shrinkage signal, we first examined CaMKII. Inhibition of CaMKII blocks LTP and long-lasting spine enlargement (Lee et al., 2009; Matsuzaki et al., 2004). If an activity-dependent shrinkage-inducing signal, and not competition for limited resources, drives heterosynaptic spine shrinkage, then blocking structural potentiation per se would not be expected to block heterosynaptic spine shrinkage. Indeed, we found that bath application of KN62 blocked HFU-induced spine enlargement without preventing heterosynaptic shrinkage of inactive spines (Figures 4A and 4B). Thus, CaMKII-mediated spine enlargement is not necessary for heterosynaptic spine shrinkage, suggesting that an activity-mediated shrinkage signal, rather than competition for limited structural resources, drives spine shrinkage during heterosynaptic structural plasticity.

If competition for limited structural resources does not drive heterosynaptic spine shrinkage, then it should be possible to observe structural potentiation of multiple stimulated spines in the absence of heterosynaptic shrinkage of unstimulated spines. To test this hypothesis, we examined the role of calcineurin. Calcineurin is a Ca^{2+}/calmodulin-dependent protein phosphatase that is required for LTD and spine shrinkage, but not for LTP (Mulkey et al., 1994; Pontrello et al., 2012; Zhou et al., 2004), and therefore could inhibit an activity-induced shrinkage signal without blocking structural potentiation of HFU-stimulated spines. Notably, we found that heterosynaptic spine shrinkage was abolished in the presence of a calcineurin inhibitor, FK506, despite that HFU-stimulated spines (on average six) underwent normal structural potentiation (Figures 4A and 4B). Thus, calcineurin signaling is necessary for heterosynaptic spine shrinkage, most likely through a mechanism that involves an activity-dependent shrinkage-inducing signal generated from stimulated spines.

How might calcineurin in the unstimulated spine be activated to promote spine shrinkage? One possibility is that HFU-stimulation could elevate calcium levels on a local dendritic segment, leading to activation of calcineurin localized in the unstimulated spine. In fact, inositol 1,4,5-trisphosphate receptor (IP_3R)-dependent propagation of calcium waves in the dendrite is required for heterosynaptic LTD (Nishiyama et al., 2000). We therefore examined the role of IP_3R and the upstream group I metabotropic glutamate receptors (mGluRs) in heterosynaptic spine shrinkage. We found that bath application of Xestospongin C, a selective IP_3R inhibitor, or 2-methyl-6-(phenylethynyl)pyridine (MPEP) and CPCCOEt, group I mGluR-specific antagonists, blocked heterosynaptic spine shrinkage without affecting structural potentiation of HFU-stimulated spines (Figures 4A and 4B). Importantly, the size of distant (>4 μm from HFU) unstimulated spines was not altered by KN62, FK506, Xestospongin C, or MPEP and CPCCOEt (Figure S4). Together, our data strongly

support an activity-induced shrinkage signal that is mediated by calcineurin, IP_3Rs, and group I mGluRs to drive heterosynaptic spine shrinkage.

DISCUSSION

Here, we show that competition between neighboring synapses drives spine shrinkage and synaptic weakening on dendrites of hippocampal pyramidal neurons. Our finding that activity-dependent potentiation of a cluster of synapses reliably leads to the shrinkage and weakening of nearby inactive synapses provides a mechanism by which synapses that are not used in a regular manner would remain immature or become eliminated while robustly active neighboring synapses would strengthen and grow (Bourne and Harris, 2011; Buffelli et al., 2003; Lee et al., 2013).

How does synaptic competition lead to spine shrinkage? Several sources have argued that competition for limited structural resources could drive heterosynaptic adjustments in synaptic weights (Fonseca et al., 2004; Miller, 1996) and parallel changes in synaptic morphology (Ramiro-Cortés et al., 2014). For example, key structural components of the synapse such as PSD-95, which has been associated with spine stability, could be redistributed by diffusion to growing synapses at the expense of their neighbors (Gray et al., 2006; Tsuriel et al., 2006). However, we found that heterosynaptic shrinkage persisted when activity-dependent spine growth was blocked by inhibiting CaMKII, demonstrating that growth of neighboring spines is not necessary to drive heterosynaptic spine shrinkage. In addition, unstimulated spines did not shrink in the presence of inhibitors of calcineurin, IP_3Rs, or group I mGluRs, despite normal growth at HFU-stimulated spines, demonstrating that structural potentiation of neighboring spines does not by itself induce shrinkage of inactive spines. Together, our results support a model in which a shrinkage signal generated in response to vigorous activity at neighboring synapses, rather than competition for limited structural resources, leads to heterosynaptic spine shrinkage and depression.

Activity-induced growth of at minimum four spines was necessary to drive heterosynaptic spine shrinkage. Why might heterosynaptic shrinkage require activation of multiple spines? An attractive hypothesis is that widespread and strong activation of multiple glutamatergic inputs is required to generate a sustained calcium elevation that spreads on local dendritic segments (Zhai et al., 2013) by calcium propagation involving IP_3Rs, leading to activation of calcineurin at nearby inactive spines. Alternatively, calcineurin activated in the HFU-stimulated spines (Fujii et al., 2013) could diffuse into adjacent regions of the dendrite, only reaching levels sufficiently high to induce spine shrinkage following activation of several neighboring spines.

What determines the spatial constraints on heterosynaptic plasticity? The limited range for heterosynaptic spine shrinkage in our studies may be determined by the extent of spread of calcium released from internal stores, which should be 3–10 μm (Malinow et al., 1994; Zhai et al., 2013), or, alternatively, by the range of diffusion of activated calcineurin. Our observation that heterosynaptic shrinkage was limited to nearby inactive spines is consistent with several electrophysiological studies on heterosynaptic depression (Lo and Poo, 1991; Royer and Paré, 2003). In contrast, some examples of heterosynaptic depression of synaptic currents can occur over relatively long distances (several hundred microns), possibly via intercellular diffusible signals (Abraham and Goddard, 1983; Chen et al., 2013; Coussens and Teyler, 1996; Huang et al., 2008; Lynch et al., 1977; Scanziani et al., 1996). Because our experiments utilized glutamate uncaging on a single dendritic segment, thus bypassing the presynaptic terminals, we conclude that the heterosynaptic shrinkage and depression observed in our studies occurs locally via a postsynaptic mechanism involving calcium wave propagation and calcineurin activation.

How might heterosynaptic plasticity contribute to experience-dependent circuit remodeling? Several studies demonstrate that synaptic potentiation occurs in a spatially clustered manner both in vitro (De Roo et al., 2008; Losonczy et al., 2008) and in vivo (Fu et al., 2012; Makino and Malinow, 2011). Heterosynaptic shrinkage and depression could drive compensatory, local homeostatic plasticity on individual dendritic segments in response to local strengthening of neighboring synapses on dendrites, thus acting to constrain total synaptic weights within stable physiological ranges (Turrigiano, 2008; Vitureira and Goda, 2013). Alternatively, heterosynaptic competition could drive the selective weakening of inactive synapses during experience-dependent neural circuit refinement. Thus, heterosynaptic shrinkage and depression could play a fundamental role in modifying synaptic structure and function in vivo via both Hebbian and homeostatic mechanisms (Goldberg et al., 2002).

EXPERIMENTAL PROCEDURES

Preparation and Transfection of Organotypic Slice Cultures

Organotypic hippocampal slice cultures were prepared from postnatal day 6 (P6)–P7 Sprague-Dawley rats, as described previously (Stoppini et al., 1991), in accordance with animal care and use guidelines of the University of California, and transfected 2–3 days (enhanced GFP [EGFP]; Clontech) or 3–4 days (tDimer-dsRed and SEP-GluA2; Kopec et al., 2006) prior to imaging using biolistic gene transfer (180 psi). A total of 20 μg of EGFP or 10 μg of tDimer-dsRed and 16 μg of SEP-GluA2 were coated onto 6–7 mg of gold particles.

Time-Lapse Two-Photon Imaging

CA1 pyramidal neurons (13–18 days in vitro [DIV]) at depths of 20–50 μm were imaged using a custom two-photon microscope with a pulsed Ti:sapphire laser (Mai Tai, Spectra Physics) tuned to 930 nm (EGFP: 0.5–1.5 mW, tDimer-dsRed and SEP-GluA2: 2–2.5 mW at the sample). The microscope and data acquisition were controlled with ScanImage (Pologruto et al., 2003). For each neuron, image stacks (512 × 512 pixels; 0.02 μm / pixel) with 1 μm z-steps were collected from one segment of secondary or tertiary basal dendrites 30–80 μm from the soma. Dendrites were imaged at 5–6 min intervals at 30°C in recirculating artificial cerebrospinal fluid (in mM: 127 NaCl, 25 $NaHCO_3$, 1.2 NaH_2PO_4, 2.5 KCl, 25 D-glucose, aerated with 95% O_2/5% CO_2, ~310 mOsm [pH 7.2]) with 2 mM $CaCl_2$, 0 mM $MgCl_2$, 2.5 mM 4-methoxy-7-nitroindolinyl-caged-L-glutamate (MNI-glutamate), and 0.001 mM tetrodotoxin (TTX).

High-Frequency Uncaging Stimulus

Uncaging of MNI-glutamate was achieved as described (Zito et al., 2009). In brief, laser pulses were delivered by parking the beam at a point ~0.5 μm from the center of the spine head. For multiple-HFU experiments, HFU consisted of 30 pulses (720 nm; 10–12 mW at the sample) of 1 ms duration

delivered at 2 Hz. For single-HFU experiments, HFU consisted of 60 pulses (720 nm; 8–9 mW at the sample) of 2 ms duration delivered at 2 Hz. To avoid confounds due to glutamate spillover, we chose unstimulated spines that were located at least 1.5 μm away from nearest stimulated spines. One dendritic region of interest was stimulated per cell.

Image Analysis

Estimated spine volume and SEP-GluA2 expression level were measured from background-subtracted and bleed-through-corrected green (EGFP or SEP-GluA2) and red (tDimer-dsRed) fluorescence images using the integrated pixel intensity of a boxed region surrounding the spine head, as described previously (Woods et al., 2011). For multiple-HFU experiments, all spines stimulated with HFU, one unstimulated spine inside the HFU cluster, and one to three unstimulated spines outside the HFU cluster were analyzed per cell; for single-HFU experiments, one stimulated spine and two unstimulated neighboring spines were analyzed per cell. Less than 15% average growth of stimulated spines was considered as HFU failure (12/61 cases). All images shown are maximum projections of 3D stacks after applying a median filter (3 × 3) to the raw image data.

Pharmacology

Stocks were prepared at 1,000× (or greater) by dissolving TTX (Calbiochem) and MPEP in water; FK506, KN62, Xestospongin C, and CPCCOEt (Tocris) in DMSO. All drugs were applied at least 20 min prior to HFU stimulation.

Statistics

All statistics were calculated across cells. Error bars represent standard error of the mean and significance was set at $p = 0.05$ (Student's two-tailed t test). Correlation was examined by Pearson's correlation. Single and double asterisks indicate $p < 0.05$ and $p < 0.01$, respectively.

SUPPLEMENTAL INFORMATION

Supplemental Information includes four figures and can be found with this article online at http://dx.doi.org/10.1016/j.celrep.2014.12.016.

AUTHOR CONTRIBUTIONS

W.C.O. and K.Z. conceived and designed the study. W.C.O. performed and analyzed all experiments except 3 HFU and mGluR inhibition experiments, which were performed and analyzed by L.K.P. W.C.O. prepared the figures and wrote the first draft of the paper. All authors revised the manuscript.

ACKNOWLEDGMENTS

We thank J. Culp for help with experiments; T. Hill for expert programming; H.J. Cheng, L. Borodinsky, J. Hell, and members of the Zito lab for valuable discussion; and H.B. Kwon and I. Stein for critical reading of the manuscript. This work was supported by the NIH (NS062736), the Whitehall Foundation (2014-05-99), and a Burroughs Wellcome Career Award in the Biomedical Sciences.

Received: March 26, 2014
Revised: October 28, 2014
Accepted: December 8, 2014
Published: December 31, 2014

REFERENCES

Abraham, W.C., and Goddard, G.V. (1983). Asymmetric relationships between homosynaptic long-term potentiation and heterosynaptic long-term depression. Nature *305*, 717–719.

Ashby, M.C., De La Rue, S.A., Ralph, G.S., Uney, J., Collingridge, G.L., and Henley, J.M. (2004). Removal of AMPA receptors (AMPARs) from synapses is preceded by transient endocytosis of extrasynaptic AMPARs. J. Neurosci. *24*, 5172–5176.

Bosch, M., and Hayashi, Y. (2012). Structural plasticity of dendritic spines. Curr. Opin. Neurobiol. *22*, 383–388.

Bourne, J.N., and Harris, K.M. (2011). Coordination of size and number of excitatory and inhibitory synapses results in a balanced structural plasticity along mature hippocampal CA1 dendrites during LTP. Hippocampus *21*, 354–373.

Buffelli, M., Burgess, R.W., Feng, G., Lobe, C.G., Lichtman, J.W., and Sanes, J.R. (2003). Genetic evidence that relative synaptic efficacy biases the outcome of synaptic competition. Nature *424*, 430–434.

Chen, J., Tan, Z., Zeng, L., Zhang, X., He, Y., Gao, W., Wu, X., Li, Y., Bu, B., Wang, W., and Duan, S. (2013). Heterosynaptic long-term depression mediated by ATP released from astrocytes. Glia *61*, 178–191.

Coussens, C.M., and Teyler, T.J. (1996). Long-term potentiation induces synaptic plasticity at nontetanized adjacent synapses. Learn. Mem. *3*, 106–114.

De Roo, M., Klauser, P., and Muller, D. (2008). LTP promotes a selective long-term stabilization and clustering of dendritic spines. PLoS Biol. *6*, e219.

Fonseca, R., Nägerl, U.V., Morris, R.G., and Bonhoeffer, T. (2004). Competing for memory: hippocampal LTP under regimes of reduced protein synthesis. Neuron *44*, 1011–1020.

Fu, M., Yu, X., Lu, J., and Zuo, Y. (2012). Repetitive motor learning induces coordinated formation of clustered dendritic spines in vivo. Nature *483*, 92–95.

Fujii, H., Inoue, M., Okuno, H., Sano, Y., Takemoto-Kimura, S., Kitamura, K., Kano, M., and Bito, H. (2013). Nonlinear decoding and asymmetric representation of neuronal input information by CaMKIIα and calcineurin. Cell Reports *3*, 978–987.

Goldberg, J., Holthoff, K., and Yuste, R. (2002). A problem with Hebb and local spikes. Trends Neurosci. *25*, 433–435.

Gray, N.W., Weimer, R.M., Bureau, I., and Svoboda, K. (2006). Rapid redistribution of synaptic PSD-95 in the neocortex in vivo. PLoS Biol. *4*, e370.

Hayama, T., Noguchi, J., Watanabe, S., Takahashi, N., Hayashi-Takagi, A., Ellis-Davies, G.C., Matsuzaki, M., and Kasai, H. (2013). GABA promotes the competitive selection of dendritic spines by controlling local Ca2+ signaling. Nat. Neurosci. *16*, 1409–1416.

Hill, T.C., and Zito, K. (2013). LTP-induced long-term stabilization of individual nascent dendritic spines. J. Neurosci. *33*, 678–686.

Holtmaat, A., and Svoboda, K. (2009). Experience-dependent structural synaptic plasticity in the mammalian brain. Nat. Rev. Neurosci. *10*, 647–658.

Holtmaat, A., Wilbrecht, L., Knott, G.W., Welker, E., and Svoboda, K. (2006). Experience-dependent and cell-type-specific spine growth in the neocortex. Nature *441*, 979–983.

Huang, Y., Yasuda, H., Sarihi, A., and Tsumoto, T. (2008). Roles of endocannabinoids in heterosynaptic long-term depression of excitatory synaptic transmission in visual cortex of young mice. J. Neurosci. *28*, 7074–7083.

Kopec, C.D., Li, B., Wei, W., Boehm, J., and Malinow, R. (2006). Glutamate receptor exocytosis and spine enlargement during chemically induced long-term potentiation. J. Neurosci. *26*, 2000–2009.

Lee, S.J., Escobedo-Lozoya, Y., Szatmari, E.M., and Yasuda, R. (2009). Activation of CaMKII in single dendritic spines during long-term potentiation. Nature *458*, 299–304.

Lee, K.J., Park, I.S., Kim, H., Greenough, W.T., Pak, D.T., and Rhyu, I.J. (2013). Motor skill training induces coordinated strengthening and weakening between neighboring synapses. J. Neurosci. *33*, 9794–9799.

Lin, D.T., and Huganir, R.L. (2007). PICK1 and phosphorylation of the glutamate receptor 2 (GluR2) AMPA receptor subunit regulates GluR2 recycling after NMDA receptor-induced internalization. J. Neurosci. *27*, 13903–13908.

Lo, Y.J., and Poo, M.M. (1991). Activity-dependent synaptic competition in vitro: heterosynaptic suppression of developing synapses. Science *254*, 1019–1022.

Losonczy, A., Makara, J.K., and Magee, J.C. (2008). Compartmentalized dendritic plasticity and input feature storage in neurons. Nature *452*, 436–441.

Lynch, G.S., Dunwiddie, T., and Gribkoff, V. (1977). Heterosynaptic depression: a postsynaptic correlate of long-term potentiation. Nature *266*, 737–739.

Makino, H., and Malinow, R. (2011). Compartmentalized versus global synaptic plasticity on dendrites controlled by experience. Neuron *72*, 1001–1011.

Malinow, R., Otmakhov, N., Blum, K.I., and Lisman, J. (1994). Visualizing hippocampal synaptic function by optical detection of Ca2+ entry through the N-methyl-D-aspartate channel. Proc. Natl. Acad. Sci. USA *91*, 8170–8174.

Matsuzaki, M., Honkura, N., Ellis-Davies, G.C., and Kasai, H. (2004). Structural basis of long-term potentiation in single dendritic spines. Nature *429*, 761–766.

Miesenböck, G., De Angelis, D.A., and Rothman, J.E. (1998). Visualizing secretion and synaptic transmission with pH-sensitive green fluorescent proteins. Nature *394*, 192–195.

Miller, K.D. (1996). Synaptic economics: competition and cooperation in synaptic plasticity. Neuron *17*, 371–374.

Mulkey, R.M., Endo, S., Shenolikar, S., and Malenka, R.C. (1994). Involvement of a calcineurin/inhibitor-1 phosphatase cascade in hippocampal long-term depression. Nature *369*, 486–488.

Nägerl, U.V., Eberhorn, N., Cambridge, S.B., and Bonhoeffer, T. (2004). Bidirectional activity-dependent morphological plasticity in hippocampal neurons. Neuron *44*, 759–767.

Nishiyama, M., Hong, K., Mikoshiba, K., Poo, M.M., and Kato, K. (2000). Calcium stores regulate the polarity and input specificity of synaptic modification. Nature *408*, 584–588.

Oh, W.C., Hill, T.C., and Zito, K. (2013). Synapse-specific and size-dependent mechanisms of spine structural plasticity accompanying synaptic weakening. Proc. Natl. Acad. Sci. USA *110*, E305–E312.

Pologruto, T.A., Sabatini, B.L., and Svoboda, K. (2003). ScanImage: flexible software for operating laser scanning microscopes. Biomed. Eng. Online *2*, 13.

Pontrello, C.G., Sun, M.Y., Lin, A., Fiacco, T.A., DeFea, K.A., and Ethell, I.M. (2012). Cofilin under control of β-arrestin-2 in NMDA-dependent dendritic spine plasticity, long-term depression (LTD), and learning. Proc. Natl. Acad. Sci. USA *109*, E442–E451.

Ramiro-Cortés, Y., Hobbiss, A.F., and Israely, I. (2014). Synaptic competition in structural plasticity and cognitive function. Philos. Trans. R. Soc. Lond. B Biol. Sci. *369*, 20130157.

Royer, S., and Paré, D. (2003). Conservation of total synaptic weight through balanced synaptic depression and potentiation. Nature *422*, 518–522.

Scanziani, M., Malenka, R.C., and Nicoll, R.A. (1996). Role of intercellular interactions in heterosynaptic long-term depression. Nature *380*, 446–450.

Stoppini, L., Buchs, P.A., and Muller, D. (1991). A simple method for organotypic cultures of nervous tissue. J. Neurosci. Methods *37*, 173–182.

Tschida, K.A., and Mooney, R. (2012). Deafening drives cell-type-specific changes to dendritic spines in a sensorimotor nucleus important to learned vocalizations. Neuron *73*, 1028–1039.

Tsuriel, S., Geva, R., Zamorano, P., Dresbach, T., Boeckers, T., Gundelfinger, E.D., Garner, C.C., and Ziv, N.E. (2006). Local sharing as a predominant determinant of synaptic matrix molecular dynamics. PLoS Biol. *4*, e271.

Turrigiano, G.G. (2008). The self-tuning neuron: synaptic scaling of excitatory synapses. Cell *135*, 422–435.

Vitureira, N., and Goda, Y. (2013). Cell biology in neuroscience: the interplay between Hebbian and homeostatic synaptic plasticity. J. Cell Biol. *203*, 175–186.

Wiegert, J.S., and Oertner, T.G. (2013). Long-term depression triggers the selective elimination of weakly integrated synapses. Proc. Natl. Acad. Sci. USA *110*, E4510–E4519.

Woods, G.F., Oh, W.C., Boudewyn, L.C., Mikula, S.K., and Zito, K. (2011). Loss of PSD-95 enrichment is not a prerequisite for spine retraction. J. Neurosci. *31*, 12129–12138.

Xu, T., Yu, X., Perlik, A.J., Tobin, W.F., Zweig, J.A., Tennant, K., Jones, T., and Zuo, Y. (2009). Rapid formation and selective stabilization of synapses for enduring motor memories. Nature *462*, 915–919.

Yang, G., Pan, F., and Gan, W.B. (2009). Stably maintained dendritic spines are associated with lifelong memories. Nature *462*, 920–924.

Zhai, S., Ark, E.D., Parra-Bueno, P., and Yasuda, R. (2013). Long-distance integration of nuclear ERK signaling triggered by activation of a few dendritic spines. Science *342*, 1107–1111.

Zhou, Q., Homma, K.J., and Poo, M.M. (2004). Shrinkage of dendritic spines associated with long-term depression of hippocampal synapses. Neuron *44*, 749–757.

Zito, K., Scheuss, V., Knott, G., Hill, T., and Svoboda, K. (2009). Rapid functional maturation of nascent dendritic spines. Neuron *61*, 247–258.

Cell Reports, Volume *10*

Supplemental Information

Heterosynaptic Structural Plasticity on Local Dendritic Segments of Hippocampal CA1 Neurons

Won Chan Oh, Laxmi Kumar Parajuli, and Karen Zito

Figure S1

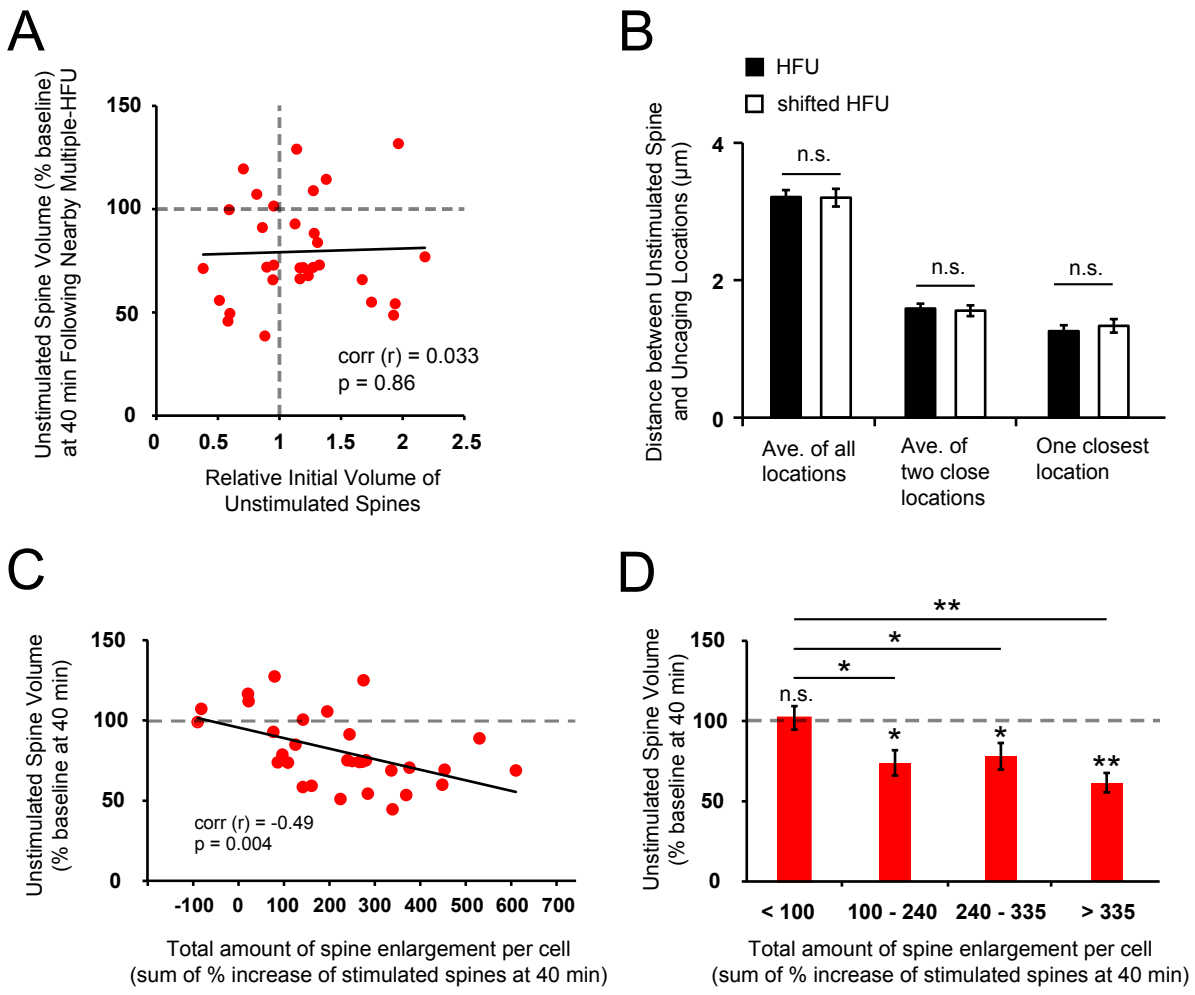

Figure S1. Characterization of heterosynaptic spine shrinkage, Related to Figure 1.
(A) Extent of shrinkage of unstimulated spines plotted against relative initial volume of unstimulated spines (normalized to the mean spine size on the same dendritic segment). Both small and large unstimulated spines shrank following potentiation of several nearby spines on the same dendritic segment (31 cells; r = 0.033, p = 0.86).
(B) Unstimulated spines in stimulated (HFU, filled black bars; n = 31 spines) and shift-stimulated (shifted HFU, open black bars; n = 15 spines) groups were equally located on average from all uncaging spots (HFU, 6.4 ± 0.1 uncaging events; shifted HFU, 6.3 ± 0.1 uncaging events; p = 0.96), from the two close uncaging spots (p = 0.77), and from the closest one uncaging location (p = 0.59).
(C) Total amount of structural potentiation of HFU-stimulated spines was inversely correlated with the extent of shrinkage of unstimulated spines (31 cells; r = -0.49, p = 0.004).
(D) Shrinkage of unstimulated spines was not observed (< 100, 8 cells, p = 0.8) on those cells for which HFU did not lead to strong potentiation; however, when the sum of HFU-induced structural potentiation of neighboring spines was higher than 100%, unstimulated spines shrank (100 - 240, 8 cells, $p < 0.05$; 240 - 335, 8 cells, $p < 0.05$; > 335, 7 cells, $p < 0.01$). Error bars represent s.e.m.; n.s., not significant.

Figure S2

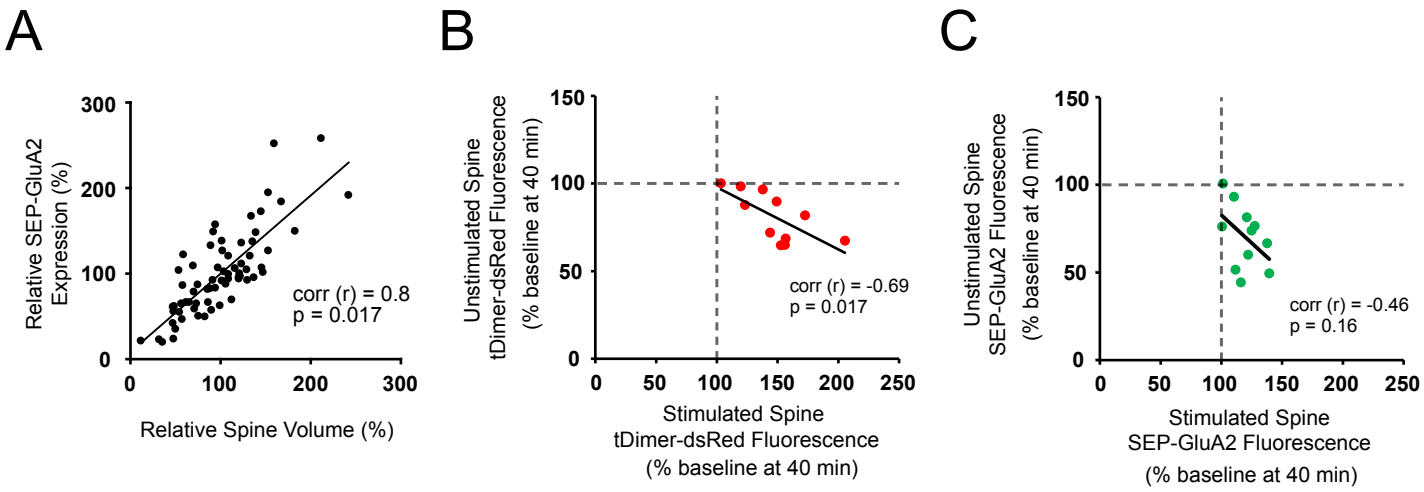

Figure S2. Inverse correlations are found in both structural and functional heterosynaptic plasticity, Related to Figure 2.

(A) Relative expression level of SEP-GluA2 plotted against relative spine volume. Scatter plot showed SEP-GluA2 expression and spine volume are highly correlated ($r = 0.8$; $p < 0.05$; $n = 68$ spines, 8 cells).

(B) An inverse correlation was found between the magnitude of structural potentiation of stimulated spines and the magnitude of shrinkage of unstimulated spines (11 cells; $r = -0.69$, $p = 0.017$).

(C) Homosynaptic increase in SEP-GluA2 fluorescence of stimulated spines was inversely correlated with heterosynaptic decrease in SEP-GluA2 fluorescence of unstimulated spines (11 cells; $r = -0.46$, $p = 0.16$).

Figure S3

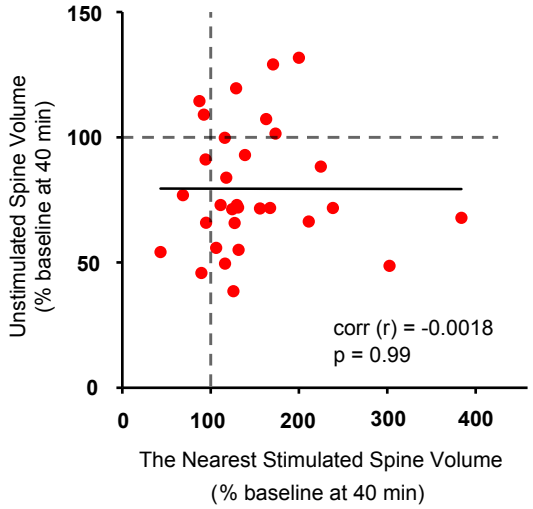

Figure S3. The magnitude of heterosynaptic spine shrinkage is not related to the extent of structural potentiation of the nearest stimulated spine, Related to Figure 3.
No correlation was observed between the magnitude of structural potentiation of the nearest stimulated spines (1 nearest stimulated spine / cell) and the magnitude of shrinkage of unstimulated spines (1 unstimulated spine / cell) on the same dendrites (31 cells; r = -0.0018, p = 0.99).

Figure S4

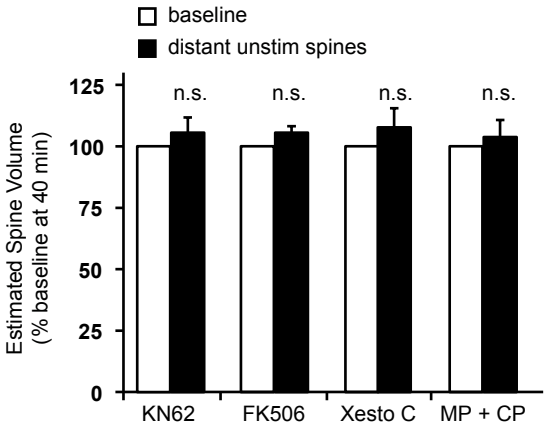

Figure S4. Neither KN62, FK506, Xestospongin C, nor MPEP and CPCCOEt alters the volume of distant unstimulated spine, Related to Figure 4.
Blocking CaMKII, calcineurin, IP_3R, or group I mGluR with bath-applied KN62, FK506, Xestospongin C, or MPEP and CPCCOEt, respectively, did not change the volume of distant unstimulated spines (KN62, n = 10 cells, p = 0.54; FK506, n = 9 cells, p = 0.49; Xesto C, n = 11 cells, p = 0.23; MP + CP, n = 15 cells, p = 0.16). Error bars represent s.e.m.; n.s., not significant.